Received: 6 October 2019 | Revised: 7 January 2020 | Accepted: 13 January 2020

DOI: 10.1111/cas.14331

ORIGINAL ARTICLE

Cancer Science WILEY

Epithelial V-like antigen 1 promotes hepatocellular carcinoma growth and metastasis via the ERBB-PI3K-AKT pathway

QianZhi Ni[1,2] | Zhenhua Chen[3] | Qianwen Zheng[2,4] | Dong Xie[2,4,5] | Jing-Jing Li[2] | Shuqun Cheng[3] | Xingyuan Ma[1]

[1]School of Biotechnology, State Key Laboratory of Bioreactor Engineering, East China University of Science and Technology, Shanghai, China

[2]CAS Key Laboratory of Nutrition, Metabolism and Food Safety, Shanghai Institute of Nutrition and Health, University of Chinese Academy of Sciences, Chinese Academy of Sciences, Shanghai, China

[3]Department of Hepatic Surgery VI, Eastern Hepatobiliary Surgery Hospital, Second Military Medical University, Shanghai, China

[4]School of Life Science and Technology, ShanghaiTech University, Shanghai, China

[5]NHC Key Laboratory of Food Safety Risk Assessment, China National Center for Food Safety Risk Assessment, Beijing, China

Correspondence
Xingyuan Ma, State Key Laboratory of Bioreactor Engineering, School of Biotechnology, East China University of Science and Technology, Shanghai 200237, China.
Email: maxy@ecust.edu.cn

Shuqun Cheng, Department of Hepatic Surgery VI, Eastern Hepatobiliary Surgery Hospital, Second Military Medical University, Shanghai 200438, China.
Email: chengshuqun@aliyun.com

Funding information
Strategic Priority Research Program of the Chinese Academy of Sciences, Grant/Award Number: XDA12010316; National Key R&D Program of China, Grant/Award Number: 2018YFC1603002, 2018YFC1604404 and 2018YFA0902804; National Natural Science Foundation of China, Grant/Award Number: 31520103907, 81730083, 31771538, 81972757, 31670944 and 81673345; Youth Innovation Promotion Association of the Chinese Academy of Sciences; Science and Technology Innovation Action Plan of Shanghai, Grant/Award Number: 17431904600

Abstract

The role of epithelial V-like antigen 1 (EVA1) has been well studied in thymic development and homostasis; however, its putative relationship with cancer remains largely unknown. Therefore, here we investigated the role of EVA1 in hepatocellular carcinoma. Interestingly, EVA1 expression was significantly increased in hepatocellular carcinoma (HCC) and was also associated with a poor prognosis and recurrence in HCC patients. Overexpression of EVA1 promoted cell growth, invasion and migration in vitro. Consistently, knockdown of EVA1 expression inhibited proliferation and migration in vitro, while repressing metastasis of HCC cells in vivo. RNA-seq analysis indicated that EVA1 is able to upregulate the expression of genes in the ERBB3-PI3K pathway. Accordingly, an increased level of AKT phosphorylation was detected in HCC cells after EVA1 overexpression. LY294002, a PI3K inhibitor, inhibited AKT phosphorylation and rescued the tumor-promoting effect of EVA1 overexpression. Altogether, the present study has revealed the oncogenic role of EVA1 during HCC progression and metastasis through the ERBB-PI3K-AKT signaling pathway, reiterating the potential use of EVA1 as a therapeutic target and/or prognostic marker for HCC.

KEYWORDS
AKT, EVA1, HCC, metastasis, PIK3R3

1 | INTRODUCTION

Hepatocellular carcinoma (HCC) is the fifth most common type of malignant tumor and a leading cause of cancer-related death worldwide.[1] HCC is a complex malignancy with various genetic abnormalities. Although HCC patients can be treated by surgical resection, radiotherapy and/or sorafenib, many HCC patients die due to recurrence, metastasis and blood vessel invasion.[2-4] Therefore, exploring the molecular mechanism of HCC tumorigenesis and metastasis may help to understand the pathogenesis of HCC and to find potential molecular targets for treatment of this malignancy.

Epithelial V-like antigen (EVA) 1 was originally identified as a member of the immunoglobulin superfamily expressed on the membrane of developing thymus epithelial cells and was strongly downregulated during thymocyte developmental progression.[5-7] It is highly homologous to the myelin protein zero and is also referred to as MPZL2. The EVA1 protein bears a characteristic V-type domain and two potential N-glycosylation sites at the extracellular domain. Several studies have indicated that EVA1 may have a role in certain malignancies, including lung,[8,9] papillary thyroid[10] and breast cancers.[11,12] Ohtsu and collegues[13] report that EVA1 might be responsible for maintaining the stem-like character of glioblastoma-initiating cells, by activating the noncanonical NF-κB signaling cascade. However, a role of EVA1 in HCC progression has not been investigated yet. In the present work, we reveal that HCC patients with high EVA1 expression have a poor prognosis and high recurrence. Furthermore, we find that EVA1 promotes cell growth and migration in vitro, while inducing metastasis in vivo. Using RNA-seq analyses, we reveal that EVA1 potentially accelerates HCC progression via ERBB-PI3K-AKT signaling. The present study reveals the function and underlying mechanisms of EVA1 in HCC, providing important insights for a potential therapeutic target and prognostic marker for this malignancy.

2 | MATERIALS AND METHODS

2.1 | Reagents

Epithelial V-like antigen 1 EVA1 and GAPDH antibodies were acquired from Proteintech (11787-1-AP); Flag antibody was purchased from Sigma (F3165); AKT and p-AKT_{473} were obtained from Cell Signaling Technology (4691 and 4051); pan-PI3K inhibitor LY294002 was purchased from MedChemExpress (HY-10108); DMEM was obtained from Gibco (12100046); FBS was acquired from Hyclone (SH30070); and Matrigel was obtained from Corning (356237).

2.2 | Cell culture and hepatocellular carcinoma samples

Cells (MHCC-97H, YY-8103, Huh7) used in this study were cultured in DMEM supplemented with 10% FBS and 1% antibiotics at 37°C and in 5% CO_2.[14] HCC tissues and paired normal tissues were collected from 220 patients at the Eastern Hepatobiliary Surgery Hospital (EHBH), Second Military Medical University (Shanghai, China). After surgical excision, all tissues were promptly frozen in liquid nitrogen and stored at −80°C. Informed written consent was obtained from all patients. All experiments were approved by the hospital's ethics committee.

2.3 | Animals

Five-week-old male BALB/c mice were housed under standard conditions. Animal protocols, based on the SIBS Guide for the Care and Use of Laboratory Animal were complied with, and the study was approved by the Animal Care and Use Committee of the Shanghai Institutes for Biological Sciences.

2.4 | Immunohistochemistry

Paraffin-embedded HCC tissues (n = 220) and normal tissues (n = 220) were analyzed by immunohistochemistry (IHC) as described previously.[15] After deparaffinization, rehydration, antigen retrieval and blocking of endogenous peroxidases, sections were washed three times in 0.01 mol/L PBS for 5 minutes and blocked for 1 hour in 5% normal goat serum, followed by incubation with anti–EVA1 (1:100) antibody at 4°C overnight. After brief washes in PBS, corresponding secondary antibodies were added, and samples were further incubated at 37°C for 1 hour. Slides were visualized after DAB staining. The staining intensity of tumor cells was scored on a scale of 0-3, with 0 indicating no staining, and 1 indicating weak staining, 2 moderate staining and 3 strong staining intensity.[16]

2.5 | RT-PCR analysis

Total RNA was extracted from HCC samples and cells using TRIzol Reagent (Invitrogen). Reverse transcription and PCR were performed as previously reported.[15] A total of 3 μg RNA was used as template for first-strand cDNA synthesis, according to the manufacturer's instructions (M-MLV Reverse transcriptase, Promega). Real-time PCR (RT-PCR) experiments were performed with Hieff qPCR SYBR Green Master Mix (Yeasen) in PIKOREAL 96 (Thermo scientific). Amplification reactions were performed in a 10-μL volume.

The PCR primers used in this study are shown (Table 1). GAPDH was used as internal control (normalizer).

2.6 | RNA sequencing

Five replicates of RNA derived from EVA1 of depleted YY-8103 and scramble control were used for RNA sequencing (RNA-seq). Analysis was performed using limma (Version 3.34.7, https://bioconductor.org/packages/release/bioc/html/limma.html).

2.7 | Plasmid transfection

Lentiviral constructs expressing EVA1 and shRNA targeting EVA1 expression were constructed as previously reported.[14] Therefore, cells were infected with Plko.1-shRNA or p23-ZsGreen-EVA1 lentivirual particles to silence or overexpress EVA1, respectively. Silenced cells were selected by puromycin treatment (2 μg/mL) for 3 days and expanded. Overexpressed cells were sorted by flow cytometry. Sequences of primers were shown in Table 1.

TABLE 1 Primer sequence

Gene	Forward	Reverse
EVA1	TGCTCTAGAATGTATGGCAAGAGCCCCGCGCTTG	CCATCGATCGTCTGTATCTTCCACAAAAACAGAG
EVA1-SH1	CCGGGTTCGACGACAATGGGACATACTCGAGTAT GTCCCATTGTCGTCGAACTTTTTG	AATTCAAAAAGTTCGACGACAATGGGACATACTCGAGTA TGTCCCATTGTCGTCGAAC
EVA1-SH2	CCGGGAAACTGCAGTTCGACGACAACTCGAGTT GTCGTCGAACTGCAGTTTCTTTTTG	AATTCAAAAAGAAACTGCAGTTCGACGACAACTCGAGT TGTCGTCGAACTGCAGTTTC
EVA1-RT	TTAATGGGACAGATGCTCGGT	AAGACACCCGGTCCTTAAACC
GAPDH-RT	ATGACCCCTTCATTGACCTCA	GAGATGATGACCCTTTTGGCT
PIK3R3-RT	TACAATACGGTGTGGAGTATGGA	TCATTGGCTTAGGTGGCTTTG
GAB1-RT	GATGGTTCGTGTTACGCAGTG	CGCTGTCTGCTACCAAGTAGAA
ERBB3-RT	GGTGATGGGGAACCTTGAGAT	CTGTCACTTCTCGAATCCACTG

2.8 | Western blot analysis

Western blot was performed as described.[16] Cultured cells or tissues were first lysed in RIPA buffer for 15 minutes on ice. Cell lysates were clarified after centrifugation at 20 800 *g* for 15 minutes. Protein concentration was determined using Bradford Reagent (Bio-Rad). Equal amounts of protein lysates were resolved by SDS-PAGE. After transferring membranes, the samples were immunoblotted with indicated primary and corresponding secondary antibodies.

2.9 | Cell growth

To assess the proliferation ability of HCC cells, crystal violet and MTT assays were performed as previously described.[15,17] MHCC-97H, YY-8103 and Huh7 cells (1000/well) were seeded in 96-well plates for various durations; 5 mg/mL MTT (20 μL/well) was added to each well and incubated for 4 hours. HCC cells were seeded at a density of 5×10^3 cells/well in six-well plates. After 7 days of cell culture, medium was removed and cells were stained with 1 mL 0.1% crystal violet solution in 20% methanol.

2.10 | Transwell assay

To evaluate the migration and invasion of HCC cells, transwell assays were performed as described.[14] For this, 2×10^5 cells were added to the upper chamber coated with or without Matrigel (BD). FBS-containing medium was loaded into bottom wells to promote migration and invasion. Cells were incubated for 36 hours. Three microscopic fields were randomly selected and cells were counted.

2.11 | Tumorigenesis in vivo

Resuspended cells were injected subcutaneously into both flanks of 5-week-old male nude mice (1×10^6 cells per injection) in accordance with AAALAC criteria. Tumor volume (cm^3) was measured every 4 days from day 7 after injection, and tumor weight was measured after the mice were killed.

2.12 | In vivo metastasis assay

Stably-transduced YY-8103 cells and respective scramble control were labeled with luciferase. A 200-μL aliquot of PBS solution containing 1×10^6 cells was delivered into 5-week-old nude mice by tail vein injection. Distant seeding lesions were monitored weekly via D-luciferin staining (150 mg/kg) using an in vivo imaging system (Xenogen). After injection of D-luciferin solution for 2 minutes, mice were placed into a light-tight chamber and monitored using a CCD camera system. The fluorescence signal from the luciferase-containing metastatic area was quantified using Living Image software.

2.13 | In vivo metastasis assay using intrahepatic injection model

Intrahepatic injection was performed as previously described.[18] Five-week-old nude mice were injected i.p. with 50 mg/kg sodium pentobarbital. Thereafter, the left lobe of mice liver was placed outside the body through a subcostal incision. A total of 5×10^5 cells were injected into hepatic lobes of nude mice. The presence of luciferase-containing HCC cells was confirmed 3 days after surgery, using the Living Image system (Xenogen). The mice were killed 8 or 12 weeks later. Metastases in injection and non–injection lobes were counted accordingly.

2.14 | Statistical analysis

Survival curves were plotted according to the Kaplan-Meier method and analyzed by log-rank test. Statistical analyses were performed using GraphPad Prism 5 and SPSS 22 (IBM) software. The results were representative of at least three independent experiments

performed in triplicate (expressed as the means ± SD). The data were analyzed using Student's *t* test. The criterion for significance was $P < .05$ for all comparisons.

3 | RESULTS

3.1 | Expression pattern and clinical significance of epithelial V-like antigen 1 in hepatocellular carcinoma

To determine the expression level of EVA1 in HCC, we performed RT-PCR to evaluate the EVA1 mRNA levels in a series of HCC tissues and matched normal hepatic tissues. EVA1 transcript levels were upregulated in 82.1% (32/39) of HCC tissues (Figure 1A). Furthermore, nine pairs of HCC tissues and adjacent normal tissues were randomly selected to detect EVA1 protein yields by western blotting. Increased EVA1 levels were found in almost all nine HCC tissues when compared with their respective normal counterparts (Figure 1B). To further confirm the expression pattern of EVA1 in HCC, the expression of EVA1 was examined by IHC staining in tissue microarrays. Consistently, the expression levels of EVA1 were significantly increased in HCC-derived tissues compared with normal tissues ($P = .0005$; Figure 1C,D), The EVA1 expression profile in HCC was similar to the one observed in lung adenocarcinoma.[9] Moreover, we analyzed the relationship between EVA1 expression and the prognosis of 220 HCC patients. In this context, we observed that high EVA1 expression levels were closely associated with poor recurrence-free survival ($P < .001$) and overall survival ($P = .001$) of HCC patients (Figure 1E,F).

According to the level of EVA1 expression, we divided HCC patients into two groups: EVA1 low (score < 79) and EVA1 high (score ≥ 79) gene expression. The relationship between EVA1 expression and the clinicopathological features of 220 HCC patients were further analyzed. As shown in Table 2, EVA1 expression level was positively associated with the presence of α-fetoprotein ($P = .004$), tumor diameter ($P = .003$), number of tumors ($P = .012$), tumor capsulation ($P = .043$), portal vein tumor thrombus (PVTT; $P = .001$) and microvascular invasion ($P = .019$; Table 2). Cox's multivariate proportional hazards model could demonstrate that some of the following factors were independent predictors of overall survival: EVA1 > 79 (hazard ratio [HR]: 2.120, 95% confidence interval [CI]: 1.358-3.309, $P = .01$), presence of PVTT (HR: 3.044, 95% CI:

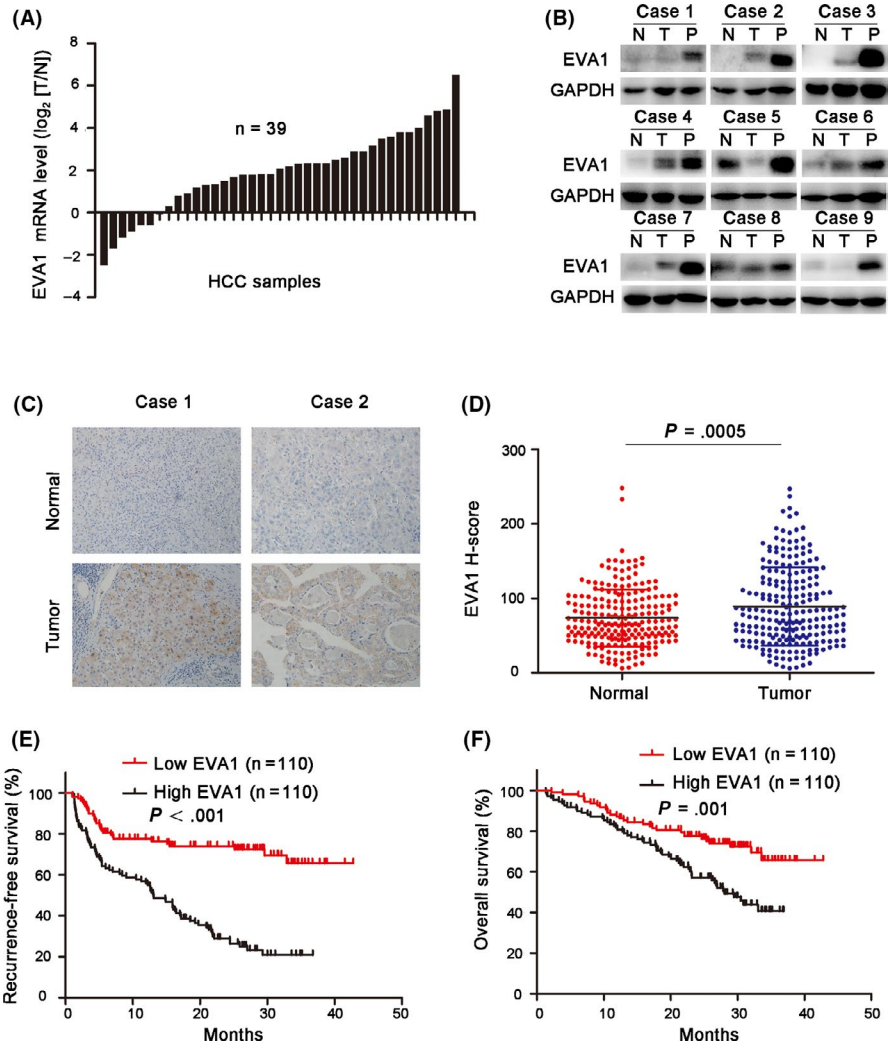

FIGURE 1 Epithelial V-like antigen 1 (EVA1) expression was upregulated in hepatocellular carcinoma (HCC) and associated with poor prognosis of patients. A, EVA1 mRNA levels in 39 pairs of tumor samples (T) and their adjacent non–carcinoma normal tissues (N) were examined by RT-PCR. B, EVA1 levels in nine pairs of N, T and portal vein tumor thrombus (PVTT) tissues (P), derived from HCC patients, were determined by western blotting. C, Representative immunohistochemistry staining of EVA1 in paired N and T tissues from 2 HCC patients, D, H-scores of EVA1 protein in N (N = 220) and T (n = 220) HCC tissues ($P = .0005$), E, F, The recurrence-free survival (EVA1 high, n = 110; EVA1 low, n = 110; $P < .001$) and overall survival (EVA1 high, n = 110; EVA1 low, n = 110; $P = .001$) of patients with high and low EVA1 expression

TABLE 2 Correlation between EVA1 expression and clinicopathological characteristics

Variables	Number	EVA1, n (%)		*P*-value
		Low expression	High expression	
Age, y				.590
<50	112	58 (52.7%)	54 (49.1%)	
≥50	108	52 (47.3%)	56 (50.9%)	
Sex				.491
Male	199	98 (89.1%)	101 (91.8%)	
Female	21	12 (10.9%)	9 (8.2%)	
HBsAg				.810
Negative	19	9 (8.2%)	10 (9.1%)	
Positive	201	101 (91.8%)	100 (90.9%)	
AFP, ng/mL				**.004**
<400	123	72 (65.5%)	51 (46.4%)	
≥400	97	38 (34.5%)	59 (53.6%)	
Total bilirubin, μmol/L				.736
≤17.1	176	89 (80.9%)	87 (79.1%)	
>17.1	44	21 (19.1%)	23 (20.9%)	
Albumin, g/L				.701
<35	7	3 (2.7%)	4 (3.6%)	
≥35	213	107 (97.3%)	106 (96.4%)	
ALT, U/L				.579
≤44	136	66 (60.0%)	70 (63.6%)	
>44	84	44 (40.0%)	40 (36.4%)	
Tumor diameter, cm				**.003**
<5	77	49 (44.5%)	28 (25.5%)	
≥5	143	61 (55.5%)	82 (74.5%)	
Number of tumors				**.012**
Single	199	105 (95.5%)	94 (85.5%)	
Multiple	21	5 (4.5%)	16 (14.5%)	
Tumor capsulation				**.043**
No	106	60 (54.5%)	46 (41.8%)	
Incomplete	51	18 (16.4%)	33 (30.0%)	
Complete	63	32 (29.1%)	31 (28.2%)	
PVTT				**.001**
Negative	184	101 (91.8%)	83 (75.5%)	
Positive	36	9 (8.2%)	27 (24.5%)	
Microvascular invasion				**.019**
Negative	133	75 (68.2%)	58 (52.7%)	
Positive	87	35 (31.8%)	52 (47.3%)	

Note: $P < .05$ is shown in bold.

Abbreviations: AFP, α-fetoprotein; ALT, Alanine Aminotransferase; EVA1, epithelial V-like antigen 1; HBsAg, Hepatitis B surface antigen; PVTT, portal vein tumor thrombus.

1.783-5.198, $P < .001$) and microvascular invasion (HR: 2.969, 95% CI: 1.925-4.580, $P < .001$; Table 3). Furthermore, the following factors were considered independent predictors of tumor recurrence in HCC patients: EVA1 > 79 (HR: 3.347, 95% CI: 2.196-5.102, $P < .001$), alanine aminotransferase (ALT) > 44 U/L (HR: 1.717,95% CI: 1.179-2.502, $P = .005$) and presence of microvascular invasion

(HR: 2.502, 95% CI: 1.713-3.652, $P < .001$; Table 4). These data revealed that EVA1 may serve as a prognostic marker in HCC and may act as a tumor promoter in HCC progression and metastasis.

3.2 | Epithelial V-like antigen 1 overexpression promoted the proliferation, invasion and migration of hepatocellular carcinoma cells in vitro

Based on the clinical data, we speculated that EVA1 may have an effect on the growth, invasion and metastasis of HCC cells. Thus, we transfected MHCC-97H, YY-8103 and Huh7 cell lines with EVA1 overexpression vector (or empty control vector) to study the function of EVA1. The endogenous expression of EVA1 in HCC cell lines was detected by western blotting (Figure S1A). The efficiency of EVA1 overexpression was evaluated by western blotting (Figures 2A and S1B). As expected, EVA1 overexpression significantly increased cell growth, which was revealed by MTT ($P < .005$; Figures 2B and S1C) and colony formation assays ($P < .05$; Figures 2C and S1D). Remarkably, forced expression of EVA1 remarkably promoted invasion ($P < .005$; Figures 2D and S1E) and migration ($P < .001$; Figures 2E and S1F) of HCC cells in vitro. These results were consistent with the increased EVA1 expression in clinical HCC samples.

3.3 | Knockdown of epithelial V-like antigen 1 expression decreased the growth and migration of hepatocellular carcinoma cells in vitro

To further confirm the effects of EVA1 in HCC cells, we knocked down EVA1 expression in YY-8103 and Huh7 cells (Figure 3A). Based on MTT assay, depletion of EVA1 significantly decreased cell proliferation ($P < .005$; Figure 3B). Consistently, reduction in colony formation was observed in EVA1 knockdown YY-8103 and Huh7 cells ($P < .005$; Figure 3C). Furthermore, EVA1 knockdown remarkably decreased HCC cell invasion ($P < .05$) and migration ($P < .005$; Figure 3D,E). These in vitro results revealed that EVA1 knockdown can effectively inhibit growth, invasion and migration of HCC cells.

3.4 | Epithelial V-like antigen 1 promoted tumorigenesis of hepatocellular carcinoma cells in vivo

To further clarify whether EVA1 could also promote the proliferation of HCC cells in vivo, scramble control and EVA1 knockdown YY-8103 and Huh7 cells were injected into the flanks of nude mice, respectively, and tumor growth was monitored (Figure 4A,B).

TABLE 3 Univariate and multivariable analysis for overall survival

	Univariate analysis		Multivariate analysis	
Variables	**HR (95% CI)**	***P*-value**	**HR (95% CI)**	***P*-value**
Age, ≥50 y	0.920 (0.608-1.392)	.694		
Sex, male	1.279 (0.619-2.645)	.506		
HBsAg, positive	1.441 (0.629-3.299)	.387		
AFP, ≥400 ng/mL	1.798 (1.173-2.756)	**.007**	1.342 (0.862-2.091)	.193
Total bilirubin, >17.1 μmol/L	1.176 (0.701-1.972)	.540		
Albumin, ≥35 g/L	0.700 (0.257-1.909)	.486		
ALT, >44 U/L	1.210 (0.795-1.841)	.375		
Tumor diameter, ≥5 cm	2.610 (1.547-4.401)	**<.001**	1.579 (0.889-2.805)	.119
Number of tumors, multiple	1.259 (0.653-2.431)	.492		
Tumor capsulation, full				
Tumor capsulation, incomplete	1.195 (0.720-1.984)	.490		
Tumor capsulation, no	1.180 (0.716-1.944)	.517		
PVTT, positive	3.044 (1.783-5.198)	**<.001**	2.033 (1.166-3.545)	**.012**
Microvascular invasion, positive	2.969 (1.925-4.580)	**<.001**	1.966 (1.207-3.201)	**.007**
EVA1, high expression	2.120 (1.358-3.309)	**.001**	1.636 (1.033-2.589)	**.036**

Note: $P < .05$ is shown in bold.

Abbreviations: AFP, α-fetoprotein; ALT, Alanine Aminotransferase; HBsAg, Hepatitis B surface antigen; PVTT, portal vein tumor thrombus.

TABLE 4 Univariate and multivariable analysis for disease-free survival

	Univariate analysis		Multivariate analysis	
Variables	**HR (95%CI)**	***P*-value**	**HR (95%CI)**	***P*-value**
Age, ≥50 y	1.206 (0.829-1.754)	.328		
Sex, male	1.709 (0.832-3.511)	.145		
HBsAg, positive	1.361 (0.662-2.796)	.402		
AFP, ≥400 ng/mL	1.614 (1.110-2.348)	**.012**	1.173 (0.791-1.738)	.428
Total bilirubin, >17.1 μmol/L	1.015 (0.630-1.633)	.953		
Albumin, ≥35 g/L	0.542 (0.134-2.196)	.391		
ALT, >44 U/L	1.717 (1.179-2.502)	**.005**	1.791 (1.179-2.721)	**.006**
Tumor diameter, ≥5 cm	2.234 (1.443-3.458)	**<.001**	1.315 (0.803-2.154)	.277
Number of tumors, multiple	1.936 (1.138-3.291)	**.015**	1.219 (0.680-2.183)	.506
Tumor capsulation, full				
Tumor capsulation, incomplete	1.551 (0.982-2.450)	.060		
Tumor capsulation, no	1.596 (1.019-2.500	**.041**	1.064 (0.619-1.829)	.822
PVTT, positive	2.083 (1.239-3.502)	**.006**	1.321 (0.664-2.629)	.427
Microvascular invasion, positive	2.502 (1.713-3.652)	**<.001**	1.888 (1.216-2.932)	**.005**
EVA1, high expression	3.347 (2.196-5.102)	**<.001**	2.697 (1.710-4.253)	**<.001**

Note: $P < .05$ is shown in bold.

Abbreviations: AFP, α-fetoprotein; ALT, alanine aminotransferase; HBsAg, Hepatitis B surface antigen; PVTT, portal vein tumor thrombus.

Tumors generated by EVA1 knockdown YY-8103 and Huh7 cells grew slower and were smaller than those generated by scramble control cells ($P < .005$; Figure 4A,B). The H&E staining of the xenograft and the immunohistochemical staining of EVA1 in tumors are shown in Figure S2A,B. These data suggested that downregulation of EVA1 impaired tumorigenesis of HCC cells in vivo, which was consistent with the function of EVA1 in vitro.

3.5 | Epithelial V-like antigen 1 promoted metastasis of hepatocellular carcinoma cells in vivo

Subsequently, we speculated whether EVA1 could enhance the metastasis of HCC cells in vivo. We used an intrahepatic metastasis mouse model to identify this hypothesis. As shown in Figure 4C, a lower foci content was detected on both injected and non–injected lobes of the nude mice injected with EVA1 knockdown YY-8103 cells, compared with those injected with scramble control cells. Furthermore, the mice bearing tumors generated by EVA1 knockdown YY-8103 cells had longer survival than control mice ($P = .04$; Figure 4C). The H&E staining of the liver and the immunohistochemical staining of EVA1 within the foci are shown in Figure S2C, which further confirmed the tumor foci and EVA1 knockdown. These results suggested that EVA1 knockdown prolonged the survival time of tumor-bearing mice by suppressing metastasis of HCC cells.

Furthermore, a tail vein injection model was used to explore the effect of EVA1 on distant seeding of HCC cells. Five weeks after injection, many metastatic foci were detected in the mice injected with YY-8103 scramble control cells, while fewer foci were observed in mice injected with EVA1 knockdown YY-8103 cells (Figure 4E). Consistent with in vitro study, these results demonstrated that EVA1 knockdown inhibited metastasis of HCC cells in vivo. Taken together, these finding suggested that EVA1 may act as a metastasis promotor in HCC.

3.6 | Epithelial V-like antigen 1 activated ERBB-PI3K-AKT signaling in hepatocellular carcinoma cells

To investigate the underlying mechanism, RNA-seq was used to identify the signaling pathways influenced by EVA1. The hierarchical clustering generated from expression of differentially expressed mRNA from EVA1 knockdown YY-8103 cells and scramble control cells disclosed distinct expression patterns of multiple mRNA between the two groups (Figure 5A). To identify pathways affected by EVA1, we used KEGG pathway enrichment to analyze the data from RNA-seq (Figure 5B). We identified expression of several fundamental genes

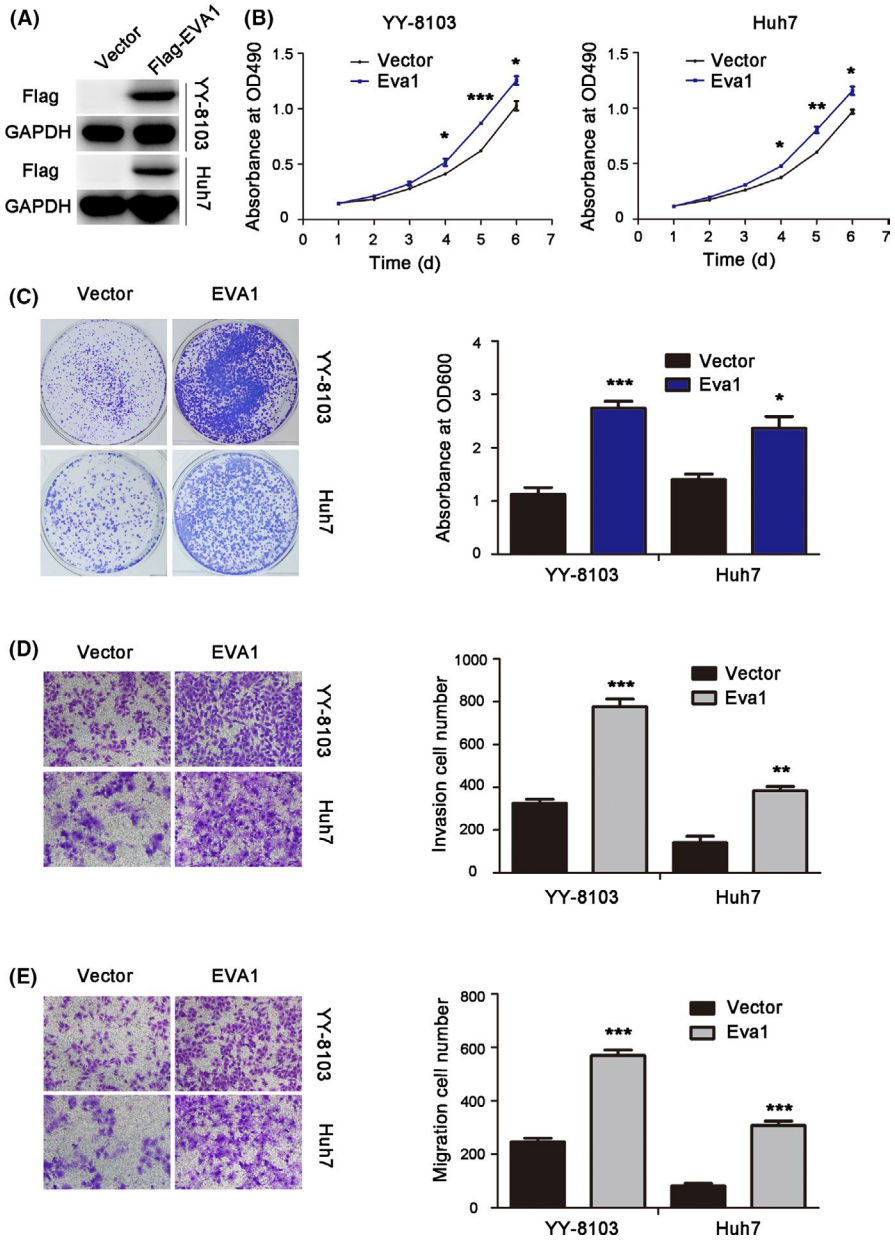

FIGURE 2 Epithelial V-like antigen 1 (EVA1) overexpression promoted growth, colony formation, invasion and migration of hepatocellular carcinoma (HCC) cells in vitro. A, Western blotting was performed to examine the protein levels of EVA1 in stably-transduced HCC cells. B, The effects of EVA1 overexpression on the viability of Huh7 and YY-8103 cells were evaluated using MTT assays. C, Crystal violet assay was used to determine the colony formation ability in HCC cells upon EVA1 overexpression. D, E, Effects of EVA1 overexpression in the invasion and migration of HCC cells were examined by transwell assay. The data are presented as the mean ± SEM. *$P < .05$; **$P < .01$; ***$P < .001$

in Notch, ERBB and TGF-b signaling pathways revealed by RNA-seq, and ERBB signaling was chosen for further study because the expression pattern of the key genes in this pathway, including ERBB3, PIK3R3 and GAB1, was consistent with our findings. In addition, ERBB3 was reported to be a promotor of hepatocarcinogenesis.[19] The mRNA expressions of PIK3R3, GAB1 and ERBB3 genes in ERBB pathway were significantly reduced in EVA1 knockdown YY-8103 cells when compared with scramble control cells. Consistently, EVA1-overexpressing YY-8103 cells exhibited a remarkable increase in mRNA expression of these genes (Figure 5C). Furthermore, we found that overexpression of EVA1 significantly elevated the level of p-AKT (Ser473) in HCC cells (Figure 5D), a well-known marker of PI3K activation. In contrast, knockdown EVA1 expression remarkably decreased the level of p-AKT (Ser473) in HCC cells (Figure 5E). To explore their relationship in the clinic, we examined the level of p-AKT (Ser473) and EVA1 in nine pairs of HCC samples (N,T,P) and their expression was quantified by Image J software. The level of p-AKT (Ser473) and EVA1 were upregulated in all nine pairs of HCC samples (Figure 5F, left). Furthermore, a positive correlation between EVA1 expression and the level of p-AKT (Ser473) was observed (Figure 5F, right, *P*-value < .0001, $r^2 = .91$). Taken together, all these results suggested that EVA1 activated the ERBB-PI3K-AKT cascade.

3.7 | LY294002, a potent PI3K inhibitor, inhibited AKT phosphorylation and rescued hepatocellular carcinoma phenotype driven by epithelial V-like antigen 1 overexpression

To further evaluate the involvement of ERBB-PI3K-Akt signaling in the tumor-promoting role of EVA1 in HCC cells, we examined whether blockade of PI3K could rescue the phenotype of EVA1-overexpression

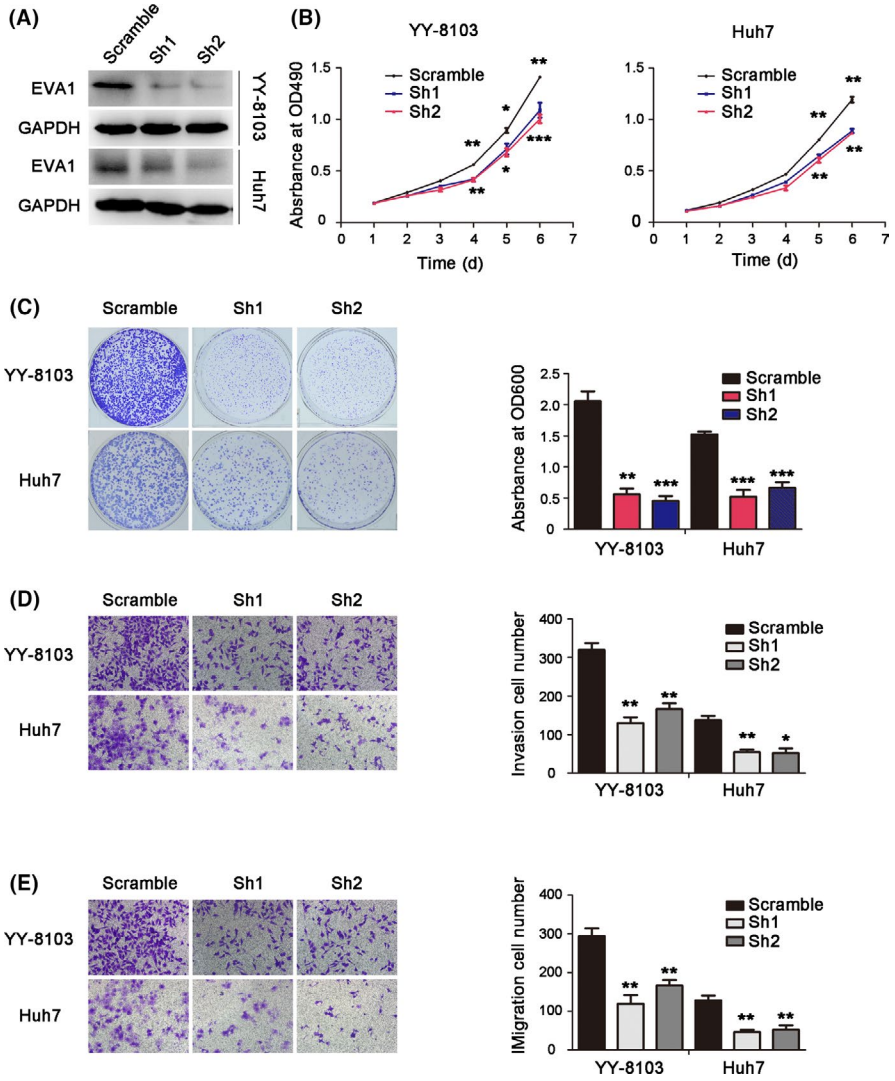

FIGURE 3 Epithelial V-like antigen 1 (EVA1) knockdown inhibited growth, colony formation, invasion and migration in hepatocellular carcinoma (HCC) cells in vitro. A, Western blotting was performed to examine the protein level of EVA1 in HCC cells after knockdown of EVA1 expression. B, MTT assay was used to assess the effect of EVA1 depletion on the viability of YY-8103 and Huh7 cells. C, Effects of EVA1 knockdown on the colony formation of HCC cells as assessed by crystal violet staining. D, E, Invasion and migration of HCC cells upon knockdown of EVA1 expression were examined by transwell assay. The data are presented as mean ± SEM. $^{*}P < .05$; $^{**}P < .01$; $^{***}P < .001$

HCC cells. Therefore, LY294002, a PI3K inhibitor,[20] was employed. LY294002 treatment significantly reduced AKT phosphorylation in EVA1-overexpression HCC cells (Figures 6A and S3A). Moreover, the inhibition of HCC cell growth, invasion and migration by EVA1 overexpression was restored upon inhibitor treatment (Figures 6B-E and S3B-E). These observations indicated that the PI3K-AKT pathway mediated the tumor-promoting effect of EVA1.

4 | DISCUSSION

Epithelial V-like antigen 1, also known as MPZL2, was first reported in thymus histogenesis.[5] A later study demonstrated expression of EVA1 on cortical and medullary epithelial cell subsets and revealed a restricted pattern of expression on CD4-CD8-double negative cell subsets.[21] Subsequent studies reported its involvement in mammary epithelial cell differentiation[12] and hearing.[22] However, its function in cancer remains largely unknown; it is reported in papillary thyroid cancer,[23] lung cancer[9] and glioblastoma[13] but not in HCC. Therefore, we explored its function and mechanism in this malignancy in the present study.

Previous studies have indicated that EVA1 is overexpressed in papillary thyroid cancer[23] and lung cancer.[24] Similar to previous reports, the present study demonstrated that EVA1 expression was higher in human HCC tissues than in matched normal tissues. HCC patients with high EVA1 expression have worse prognoses and higher recurrence rates than those with low EVA1 expression. Moreover, based on multivariate analysis, the present study demonstrated that EVA1 overexpression, tumor diameter, positive PVTT and microvascular invasion were independent and significant risk factors for survival or recurrence. Taken together, the present study demonstrated that EVA1 could be a dependable biomarker of HCC.

Hepatocellular carcinoma tends to invade the intrahepatic vasculature, especially through the portal vein.[25] Frequent intrahepatic and extrahepatic metastases of HCC are responsible for the poor clinical prognosis of HCC patients.[26] Previous studies have indicated that EVA1 is essential for epithelial differentiation of immortalized human mammary epithelial cells.[12] Additional work has reported that EVA1 may have a function in lung cancer development as a cell adhesion molecule.[8] However, whether EVA1 has a metastatic function in cancer has not been confirmed. The present

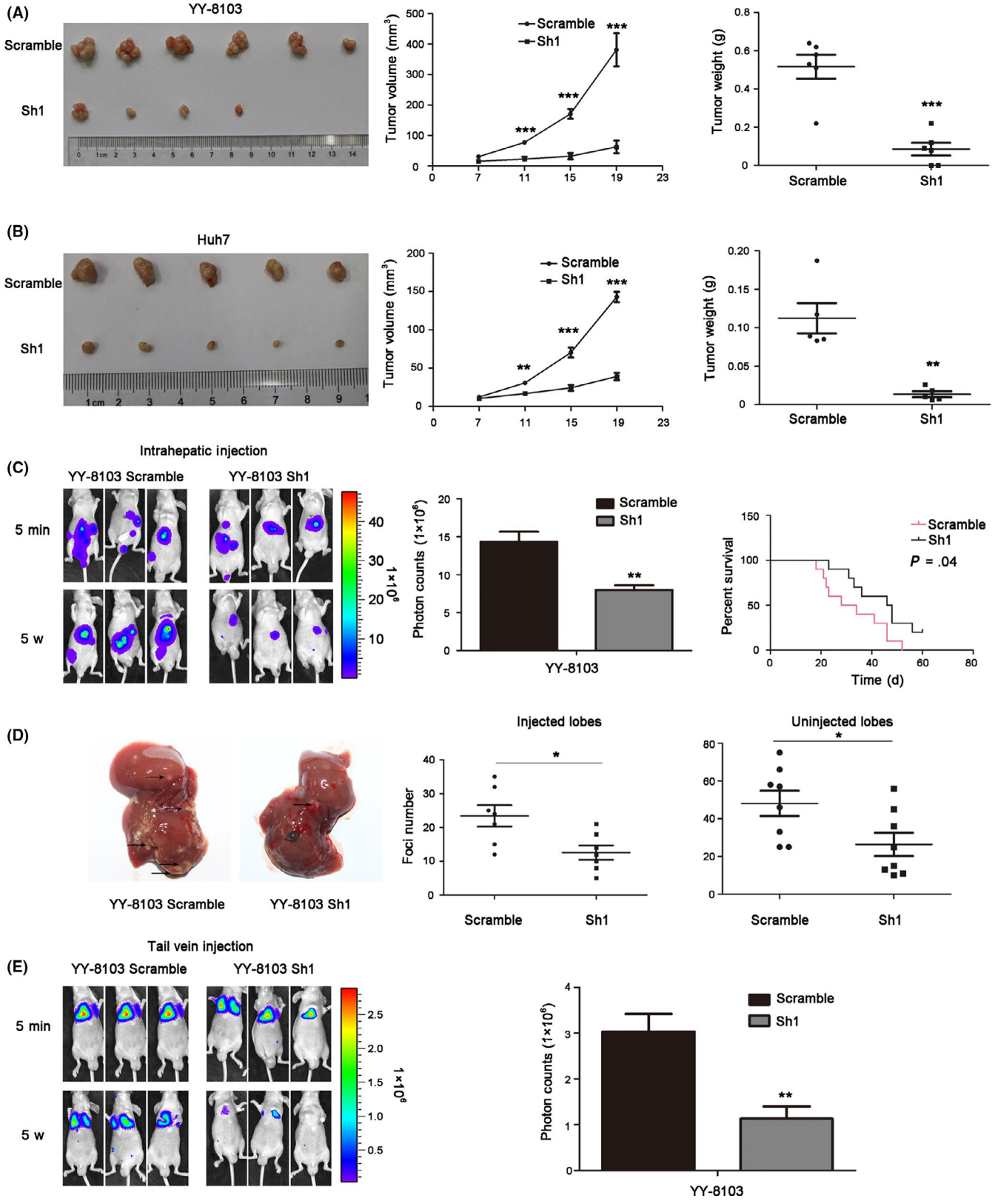

FIGURE 4 Epithelial V-like antigen 1 (EVA1) knockdown suppressed the tumorigenesis and metastasis of hepatocellular carcinoma (HCC) cells in vivo. A, B, Imaging, growth curves (cm^3) and weight (g) of the tumors generated after injection of scramble or EVA1 knockdown YY-8103 cells and Huh7 cells. C, Imaging, photon counts and survival curve of the intrahepatic metastasis of scramble and EVA1 knockdown YY-8103 cells. D, Foci number of injection and non–injection lobes of intrahepatic metastasis mouse model, using stably-transduced HCC cells. E, Fluorescence of metastases generated by distant seeding after tail vein injection with EVA1 knockdown or scramble HCC cells in mice. Each bar represents the mean ± SD. *P < .05; **P < .01; ***P < .001

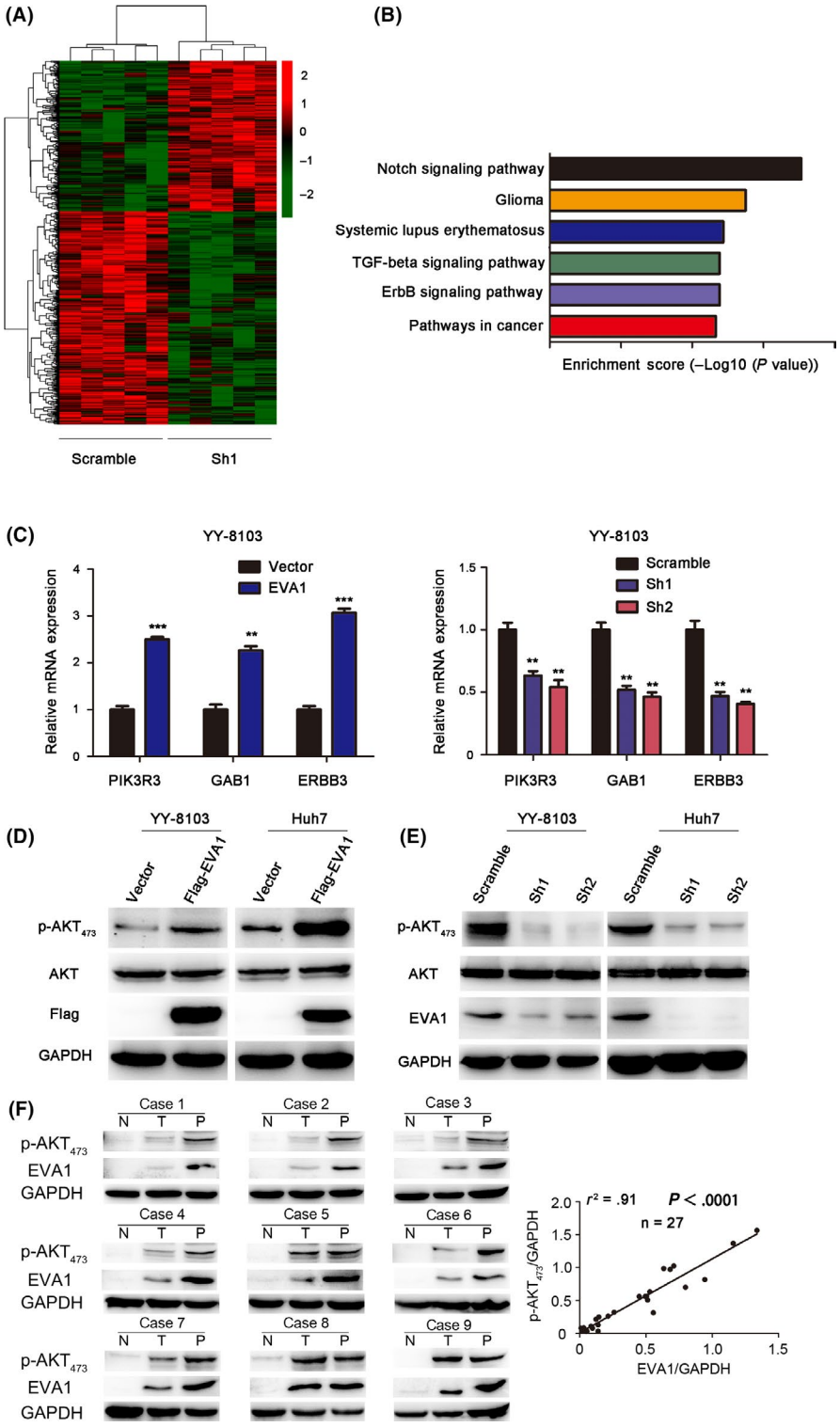

FIGURE 5 Epithelial V-like antigen 1 (EVA1) activates the ERBB3-PI3K-AKT signaling pathway in hepatocellular carcinoma (HCC) cells. A, A Hierarchical clustering generated from differentially expressed mRNA upon knockdown of EVA1 expression in YY-8103 cells and scramble cells group, B, KEGG enrichment plot based on RNA-seq results, C, RT-PCR was performed to validate the effect of EVA1 on the ERBB-PI3K-AKT pathway in YY-8103 cells, D, E, Overexpression and knockdown of EVA1, respectively, activated and suppressed the level of AKT phosphorylation in YY-8103 and Huh7 cells, as assessed by western blotting. F, Western blotting analysis of EVA1 and AKT phosphorylation in nine pairs of HCC samples (left) abd linear regression analysis showing the positive correlation between p-AKT$_{473}$ and EVA1 (right)

study revealed that EVA1 is capable of promoting invasion and migration of HCC cells. Furthermore, an intrahepatic metastasis mouse model was used to clarify the effect of EVA1 on intrahepatic metastasis, while a tail vein injection model was used to explore the effect of EVA1 on the distant seeding of HCC cells. Collectively, these data revealed that EVA1 promoted metastasis of HCC cells in vitro and in vivo. Taken together, here we confirmed that EVA1 has a significant promoting role in the hepatic metastases of HCC.

In this study, we explored the mechanism underlying the tumor-promoting effect of EVA1 by RNA-seq. The RNA-seq analysis revealed that the function of EVA1 in HCC may be associated with the Notch signaling pathway, the TGF-beta signaling pathway and the ERBB signaling pathway, which was consistent with previous studies reporting its relationship with Notch signaling.[27] Here, we chose ERBB signaling for further study because the expression pattern of the key genes in this pathway was consistent with

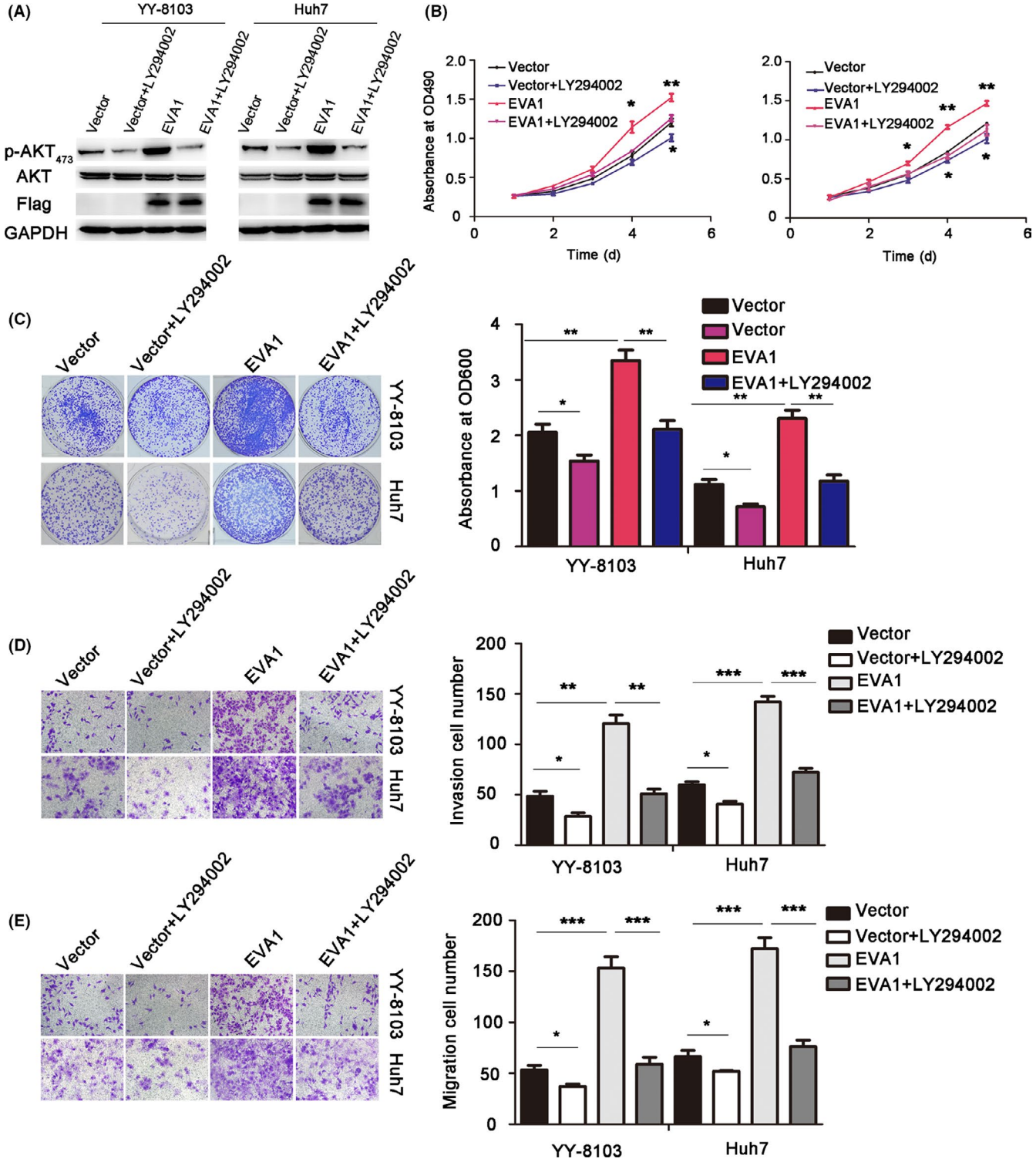

FIGURE 6 LY294002, a PI3K inhibitor, suppressed the level of AKT phosphorylation and rescued hepatocellular carcinoma (HCC) phenotype driven by epithelial V-like antigen 1 (EVA1) overexpression. A, LY294002 suppressed the level of AKT phosphorylation in YY-8103 and Huh7 cells with EVA1 overexpressing assessed by western blotting. B, MTT assays were used to evaluate the effects of suppressing the level of phosphorylation on the viability of YY-8103 and Huh7 cells. C, Crystal violet assays were used to assess the effects of inhibiting AKT phosphorylation on the colony formation ability of HCC cells. D, Effects of suppressing the level of AKT phosphorylation on the invasion and migration (E) of HCC cells were evaluated by transwell assay. The data are presented as the mean ± SEM. *P < .05; **P < .01; ***P < .001

the observed phenotype. High expression of ERBB3 in certain human cancers led early on to the suggestion that it could be a therapeutic target.[28] ERBB3 was reported to have an oncogenic role in HCC.[29] The most fully studied target of ERBB3 is the p85 regulatory subunit of PI3K (PI3KR). Moreover, Jones et al[30] found that both SH2 groups in each of the three PI3KR isoforms bound

with moderate or high affinity at multiple sites in ERBB3, including PIK3R3. PIK3R3 is associated with the activation of the class IA PI3K complex, as one of its regulatory subunits.[31] PIK3R3 promotes tumor growth or metastasis in esophageal squamous cell carcinoma,[32] glioma,[33] HCC,[31,34,35] ovarian cancer,[36] gastric cancer,[37] colorectal cancer[38] and pancreatic cancer.[39] Another identified candidate gene in ERBB signaling is GAB1, a docking protein that recruits phosphatidylinositol-3 kinase (PI-3 kinase) and other effector proteins in response to the activation of many receptor tyrosine kinases.[40] Here we found that EVA1 regulated the mRNA level of ERBB3, PIK3R3 and GAB1, the genes whose protein product existed in the ERBB signaling transduction complex, indicating its modulation of the ERBB-PI3K-AKT pathway. Consistently, the present study demonstrated that depletion of EVA1 expression significantly suppressed the level of AKT phosphorylation and EVA1 overexpression remarkably promoted the level of AKT phosphorylation in HCC cells, which further confirmed the impact on ERBB-PI3K-Akt signaling by EVA1. In addition, LY294002, a PI3K inhibitor, significantly reduced the level of AKT phosphorylation and inhibited HCC cell growth, invasion and migration in EVA1-overexpressing cells, which rescued the phenotype induced by forced expression of EVA1. The accumulating evidence suggested that EVA1 exerted a tumor-promoting effect via the ERBB-PI3K-AKT pathway. Protein interaction data from Uniprot (https://www.uniprot.org) revealed that EVA1 potentially interacts with ERBB1 and ERBB2.[41] EVA1 is a transmembrane protein. In addition, ERBB3 itself has impaired tyrosine kinase activity and needs a dimerization partner to become phosphorylated and to acquire signaling potential. It is possible that EVA1 interacts with ERBB members to regulate downstream signaling. Further study is required to identify this interesting hypothesis.

It is noteworthy that the mRNA level of ERBB3, PIK3R3 and GAB1, the proteins in the ERBB3 signaling complex, was influenced by EVA1. The transcription of ERBB3 was regulated by several transcriptional factors, including SOX10[42] and FoxO3a.[43] It was reported that transcription of GAB1 could be regulated by RARα[44] and several microRNA, such as miR-150[45] and miR-29a-3p.[46] As for PIK3R3, its transcription was reported to be regulated by SREBP1c[47] and TGF-β signaling.[48] Further research is needed to interpret the impact of EVA1 on the expression of ERBB3, PIK3R3 and GAB1.

In summary, the present study demonstrated the significant role of EVA1 in tumor progression, recurrence and prognosis of HCC, and further correlated these effects with an underlying mechanism involving the ERBB-PI3K-AKT pathway. As such, EVA1 acts as an oncogene by promoting tumor progression and metastasis in HCC. Taken together, we strongly believe that EVA1 is a potential prognostic indicator and molecular target for HCC therapies.

ACKNOWLEDGMENTS

This work was supported by: the "Personalized Medicines-Molecular Signature-based Drug Discovery and Development," Strategic Priority Research Program of the Chinese Academy of Sciences (Grant No. XDA12010316), the National Key R&D Program of China (2018YFC1603002 and 2018YFC1604404) and the National Natural Science Foundation of China (31520103907 and 81730083) to Dong Xie; the National Natural Science Foundation of China (31771538 and 81972757), the Youth Innovation Promotion Association of the Chinese Academy of Sciences fund and the Sanofi-SIBS 2018 Young Faculty Award to Jing-Jing Li; and the National Key Research and Development Project of China (2018YFA0902804), the National Natural Science Foundation (31670944 and 81673345) and the Science and Technology Innovation Action Plan of Shanghai (17431904600). We thank the New World Group for their Charitable Foundation to establish the Institute for Nutritional Sciences, SIBS, CAS-New World Joint Laboratory, which have given full support to this study.

CONFLICT OF INTEREST

The authors have no conflict of interest to declare.

ORCID

QianZhi Ni https://orcid.org/0000-0002-4659-7696
Shuqun Cheng https://orcid.org/0000-0001-6760-7470
Xingyuan Ma https://orcid.org/0000-0002-8740-7748

REFERENCES

1. Ferlay J, Soerjomataram I, Dikshit R, et al. Cancer incidence and mortality worldwide: sources, methods and major patterns in GLOBOCAN 2012. *Int J Cancer*. 2015;136:E359-E386.
2. Yu WB, Rao A, Vu V, Xu L, Rao JY, Wu JX. Management of centrally located hepatocellular carcinoma: update 2016. *World J Hepatol*. 2017;9:627-634.
3. Omata M, Cheng A-L, Kokudo N, et al. Asia-Pacific clinical practice guidelines on the management of hepatocellular carcinoma: a 2017 update. *Hepatol Int*. 2017;11(4):317-370.
4. Khemlina G, Ikeda S, Kurzrock R. The biology of hepatocellular carcinoma: implications for genomic and immune therapies. *Mol Cancer*. 2017;16:149.
5. Guttinger M, Sutti F, Panigada M, et al. Epithelial V-like antigen (EVA), a novel member of the immunoglobulin superfamily, expressed in embryonic epithelia with a potential role as homotypic adhesion molecule in thymus histogenesis. *J Cell Biol*. 1998;141:1061-1071.
6. Iacovelli S, Iosue I, Di Cesare S, Guttinger M. Lymphoid EVA1 expression is required for DN1-DN3 thymocytes transition. *PLoS ONE*. 2009;4:e7586.
7. DeMonte L, Porcellini S, Tafi E, et al. EVA regulates thymic stromal organisation and early thymocyte development. *Biochem Biophys Res Commun*. 2007;356:334-340.
8. Difilippantonio S, Chen Y, Pietas A, et al. Gene expression profiles in human non–small and small-cell lung cancers. *Eur J Cancer*. 2003;39:1936-1947.
9. Davidson B, Stavnes HT, Risberg B, et al. Gene expression signatures differentiate adenocarcinoma of lung and breast origin in effusions. *Hum Pathol*. 2012;43:684-694.
10. Hucz J, Kowalska M, Jarzab M, Wiench M. Gene expression of metalloproteinase 11, claudin 1 and selected adhesion related genes in papillary thyroid cancer. *Endokrynol Pol*. 2006;57(Suppl. A):18-25.
11. Singh R, Parveen M, Basgen JM, et al. Increased expression of beige/brown adipose markers from host and breast cancer cells influence xenograft formation in mice. *Mol Cancer Res*. 2016;14:78-92.
12. Ramena G, Yin Y, Yu Y, Walia V, Elble RC. CLCA2 interactor EVA1 is required for mammary epithelial cell differentiation. *PLoS ONE*. 2016;11:e0147489.

13. Ohtsu N, Nakatani Y, Yamashita D, Ohue S, Ohnishi T, Kondo T. Eva1 maintains the stem-like character of glioblastoma-initiating cells by activating the noncanonical NF-kappaB signaling pathway. *Cancer Res*. 2016;76:171-181.
14. Jiang H, Ma N, Shang Y, et al. Triosephosphate isomerase 1 suppresses growth, migration and invasion of hepatocellular carcinoma cells. *Biochem Biophys Res Commun*. 2017;482:1048-1053.
15. Deng YZ, Yao F, Li JJ, et al. RACK1 suppresses gastric tumorigenesis by stabilizing the beta-catenin destruction complex. *Gastroenterology*. 2012;142:812-823.e15.
16. Li J-J, Yin H-K, Guan D-X, et al. Chemerin suppresses hepatocellular carcinoma metastasis through CMKLR1-PTEN-Akt axis. *Br J Cancer*. 2018;118:1337-1348.
17. Feng YX, Zhao JS, Li JJ, et al. Liver cancer: EphrinA2 promotes tumorigenicity through Rac1/Akt/NF-kappaB signaling pathway. *Hepatology*. 2010;51:535-544.
18. Tada H, Maron DJ, Choi EA, et al. Systemic IFN-beta gene therapy results in long-term survival in mice with established colorectal liver metastases. *J Clin Invest*. 2001;108:83-95.
19. Scheving LA, Zhang X, Stevenson MC, et al. Loss of hepatocyte ERBB3 but not EGFR impairs hepatocarcinogenesis. *Am J Physiol Gastrointest Liver Physiol*. 2015;309:G942-G954.
20. Jiang H, Fan D, Zhou G, Li X, Deng H. Phosphatidylinositol 3-kinase inhibitor (LY294002) induces apoptosis of human nasopharyngeal carcinoma in vitro and in vivo. *J Exp Clin Cancer Res*. 2010;29:34.
21. Garabatos N, Blanco J, Fandos C, et al. A monoclonal antibody against the extracellular domain of mouse and human epithelial V-like antigen 1 reveals a restricted expression pattern among CD4- CD8- thymocytes. *Monoclon Antib Immunodiagn Immunother*. 2014;33:305-311.
22. Wesdorp M, Murillo-Cuesta S, Peters T, et al. MPZL2, encoding the epithelial junctional protein myelin protein zero-like 2, is essential for hearing in man and mouse. *Am J Hum Genet*. 2018;103:74-88.
23. Jarząb B, Wiench M, Fujarewicz K, et al. Gene expression profile of papillary thyroid cancer: sources of variability and diagnostic implications. *Cancer Res*. 2005;65:1587-1597.
24. Xu BB, Gu ZF, Ma M, Wang JY, Wang HN. MicroRNA-590-5p suppresses the proliferation and invasion of non–small cell lung cancer by regulating GAB1. *Eur Rev Med Pharmacol Sci*. 2018;22:5954-5963.
25. Llovet JM, Bustamante J, Castells A, et al. Natural history of untreated nonsurgical hepatocellular carcinoma: rationale for the design and evaluation of therapeutic trials. *Hepatology*. 1999;29:62-67.
26. Aldrighetti L, Pulitano C, Catena M, et al. Liver resection with portal vein thrombectomy for hepatocellular carcinoma with vascular invasion. *Ann Surg Oncol*. 2009;16:1254.
27. Tydell CC, David-Fung ES, Moore JE, Rowen L, Taghon T, Rothenberg EV. Molecular dissection of prethymic progenitor entry into the T lymphocyte developmental pathway. *J Immunol*. 2007;179:421-438.
28. Gullick WJ. The c-erbB3/HER3 receptor in human cancer. *Cancer Surv*. 1996;27:339-349.
29. Shi D-M, Li L-X, Bian X-Y, et al. miR-296-5p suppresses EMT of hepatocellular carcinoma via attenuating NRG1/ERBB2/ERBB3 signaling. *J Exp Clin Cancer Res*. 2018;37:294.
30. Jones RB, Gordus A, Krall JA, MacBeath G. A quantitative protein interaction network for the ErbB receptors using protein microarrays. *Nature*. 2006;439:168-174.
31. Lu J, Tang L, Xu Y, et al. Mir-1287 suppresses the proliferation, invasion, and migration in hepatocellular carcinoma by targeting PIK3R3. *J Cell Biochem*. 2018;119:9229-9238.
32. Nicolau-Neto P, Da Costa NM, de Souza Santos PT, et al. Esophageal squamous cell carcinoma transcriptome reveals the effect of FOXM1 on patient outcome through novel PIK3R3 mediated activation of PI3K signaling pathway. *Oncotarget*. 2018;9:16634-16647.
33. Zhu Y, Zhao H, Rao M, Xu S. MicroRNA-365 inhibits proliferation, migration and invasion of glioma by targeting PIK3R3. *Oncol Rep*. 2017;37:2185-2192.
34. Liu K, Li X, Cao Y, Ge Y, Wang J, Shi B. MiR-132 inhibits cell proliferation, invasion and migration of hepatocellular carcinoma by targeting PIK3R3. *Int J Oncol*. 2015;47:1585-1593.
35. Song Y, He S, Zhuang J, et al. MicroRNA601 serves as a potential tumor suppressor in hepatocellular carcinoma by directly targeting PIK3R3. *Mol Med Rep*. 2019;19:2431-2439.
36. Dong S, Wang R, Wang H, et al. HOXD-AS1 promotes the epithelial to mesenchymal transition of ovarian cancer cells by regulating miR-186-5p and PIK3R3. *J Exp Clin Cancer Res*. 2019;38:110.
37. Sun J, Fu L. IL-6 promotes gastric cancer cell proliferation and EMT through regulating miR-152/PIK3R3 pathway. *Zhong Nan Da Xue Xue Bao Yi Xue Ban*. 2017;42:1241-1247.
38. Wang G, Yang X, Li C, Cao X, Luo X, Hu J. PIK3R3 induces epithelial-to-mesenchymal transition and promotes metastasis in colorectal cancer. *Mol Cancer Ther*. 2014;13:1837-1847.
39. Peng YP, Zhu Y, Yin LD, et al. PIK3R3 promotes metastasis of pancreatic cancer via ZEB1 induced epithelial-mesenchymal transition. *Cell Physiol Biochem*. 2018;46:1930-1938.
40. Aasrum M, Odegard J, Sandnes D, Christoffersen T. The involvement of the docking protein Gab1 in mitogenic signalling induced by EGF and HGF in rat hepatocytes. *Biochim Biophys Acta*. 2013;1833:3286-3294.
41. Yao Z, Darowski K, St-Denis N, et al. A global analysis of the receptor tyrosine kinase-protein phosphatase interactome. *Mol Cell*. 2017;65:347-360.
42. Prasad MK, Reed X, Gorkin DU, et al. SOX10 directly modulates ERBB3 transcription via an intronic neural crest enhancer. *BMC Dev Biol*. 2011;11:40.
43. Garrett JT, Olivares MG, Rinehart C, et al. Transcriptional and posttranslational up-regulation of HER3 (ErbB3) compensates for inhibition of the HER2 tyrosine kinase. *Proc Natl Acad Sci USA*. 2011;108:5021-5026.
44. Laursen KB, Wong PM, Gudas LJ. Epigenetic regulation by RARalpha maintains ligand-independent transcriptional activity. *Nucleic Acids Res*. 2012;40:102-115.
45. Mraz M, Chen L, Rassenti LZ, et al. miR-150 influences B-cell receptor signaling in chronic lymphocytic leukemia by regulating expression of GAB1 and FOXP1. *Blood*. 2014;124:84-95.
46. Shao NY, Wang DX, Wang Y, et al. MicroRNA-29a-3p downregulation causes Gab1 upregulation to promote glioma cell proliferation. *Cell Physiol Biochem*. 2018;48:450-460.
47. Kallin A, Johannessen LE, Cani PD, et al. SREBP-1 regulates the expression of heme oxygenase 1 and the phosphatidylinositol-3 kinase regulatory subunit p55 gamma. *J Lipid Res*. 2007;48:1628-1636.
48. Wang G, Yang X, Jin Y, et al. TGF-beta regulates the proliferation of lung adenocarcinoma cells by inhibiting PIK3R3 expression. *Mol Carcinog*. 2015;54(Suppl. 1):E162-E171.

SUPPORTING INFORMATION

Additional supporting information may be found online in the Supporting Information section.

How to cite this article: Ni Q, Chen Z, Zheng Q, et al. Epithelial V-like antigen 1 promotes hepatocellular carcinoma growth and metastasis via the ERBB-PI3K-AKT pathway. *Cancer Sci*. 2020;111:1500–1513. https://doi.org/10.1111/cas.14331